Newly identified protein Imi1 affects mitochondrial integrity and glutathione homeostasis in *Saccharomyces cerevisiae*

Piotr Kowalec[1], Marcin Grynberg[1], Beata Pająk[2,3], Anna Socha[4,5], Katarzyna Winiarska[6], Jan Fronk[4], Anna Kurlandzka[1*]

[1]Institute of Biochemistry and Biophysics, Polish Academy of Sciences, Warsaw, Poland
pkowalec@ibb.waw.pl; mr.cingg@gmail.com; ania218@ibb.waw.pl

[2]Electron Microscopy Platform, Mossakowski Medical Research Centre, Polish Academy of Sciences, Warsaw, Poland
and
[3]Department of Physiological Sciences, Faculty of Veterinary Medicine, Warsaw University of Life Sciences (SGGW), Warsaw, Poland
bepaj@wp.pl

[4] Department of Molecular Biology, Institute of Biochemistry, Faculty of Biology, University of Warsaw, Warsaw, Poland
anna.socha@sjc.ox.ac.uk; fronk@biol.uw.edu.pl

[*]**Correspondence:** Anna Kurlandzka
Institute of Biochemistry and Biophysics, Polish Academy of Sciences,
Pawinskiego 5A, 02-106 Warsaw, Poland,
Tel.:+48 22 5921318, fax: +48 22 6584636
E-mail: ania218@ibb.waw.pl

[5]Present address:
Department of Biochemistry, University of Oxford, South Parks Road, Oxford OX1 3QU, UK

[6] Department of Metabolic Regulation, Institute of Biochemistry, Faculty of Biology,
University of Warsaw, Warsaw, Poland
k.winiarska@biol.uw.edu.pl

Running title

Imi1 in glutathione homeostasis and mitochondrial integrity

Keywords: Yeast, Glutathione, Mitochondria, Phytochelatin, *IMI1* gene

Abstract

Glutathione homeostasis is crucial for cell functioning. We describe a novel Imi1 protein of *Saccharomyces cerevisiae* affecting mitochondrial integrity and involved in controlling glutathione level. Imi1 is cytoplasmic and, except for its N-terminal Flo11 domain, has a distinct solenoid structure. A lack of Imi1 leads to mitochondrial lesions comprising aberrant morphology of cristae and multifarious mtDNA rearrangements and impaired respiration. The mitochondrial malfunctioning is coupled to significantly decrease of the level of intracellular reduced glutathione without affecting oxidized glutathione, which decreases the reduced/oxidized glutathione ratio. These defects are accompanied by decreased cadmium sensitivity and increased phytochelatin-2 level.

Introduction

A precisely controlled redox state is crucial for the correct execution of numerous biological processes, the majority of which require reducing conditions. In such conditions sulfhydryl groups are reduced and key enzymes and non-enzymatic proteins remain functional. In eukaryotic cells, highly reducing environments prevail in the cytosol, mitochondrial matrix, and peroxisomes (Ayer *et al*., 2014).

Glutathione (γ-L-glutamyl-L-cysteinylglycine), a redox buffer and protectant, is the best-known and most abundant non-enzymatic component of the antioxidant defence system. Glutathione is present within the cell in both reduced (GSH) and oxidized (GSSG) forms (Schafer & Buettner, 2001). GSSG can be reduced to GSH by glutathione reductase and by the thioredoxin or glutaredoxin systems (Tan *et al*., 2010; Luikenhuis *et al*., 1998; Ströher & Millar, 2012). Inside the cell glutathione cycles between GSH and GSSG, forming a redox couple that has a major effect on the overall redox status. Changes in the GSH/GSSG ratio are routinely used as indicators of perturbation of the intracellular redox state (Meister &

Anderson, 1983; Schafer & Buettner, 2001; Ostergaard *et al*., 2004). Glutathione plays several important roles in the cell (Burhans & Heintz 2009; Ayer *et al*., 2010). Its homeostasis is critical for protection of mitochondria (including the maintenance of their genome) from the deleterious effects of reactive oxygen species (ROS) abundantly produced by the electron transport chain. Consequently, glutathione deficiency leads to mitochondrial damage and subsequent cell apoptosis (Meister, 1995; Turrens, 2003). Glutathione also has other activities, including the formation of mixed disulfides with redox-active protein thiols, which can modulate the properties of a variety of cellular targets (Handy & Loscalzo, 2012).

Glutathione metabolism in the yeast *Saccharomyces cerevisiae* is well characterized (Jamieson, 1998; Bachhawat *et al*., 2009; Petrova & Kujumdzieva, 2010). *S. cerevisiae* cells with disrupted glutathione biosynthesis exhibit reduced tolerance to a wide range of stress conditions (Izawa *et al*., 1995; Turton *et al*., 1997; Grant *et al*., 1998) and an increased rate of apoptosis (Madeo *et al*., 1999).

Although the genome of *S. cerevisiae* was the first eukaryotic one to be sequenced (Goffeau *et al*., 1996), a substantial fraction of the ca. 6000 of its open reading frames still lack an assigned molecular function. Here we characterize a newly identified protein encoded by a gene which we named *IMI1* (GenBank accession number: KC256787.1). Deletion of the *IMI1* gene caused degeneration of mitochondrial cristae and mtDNA rearrangements leading to respiratory deficiency, and a decreased intracellular GSH level. Surprisingly, those defects were accompanied by an increased tolerance of the *imi1Δ* mutant to cadmium, which correlated with an elevated level of phytochelatin-2. Thus, the Imi1 protein is a novel factor affecting mitochondral integrity and glutathione homeostasis and therby modulating cell functioning.

Materials and methods

Nomenclature, strains, media, growth conditions

Standard genetic nomenclature is used to designate wild-type alleles (e.g., *IMI1*, *URA3*), recessive mutant alleles (e.g., *ade2-1*), and disruptants or deletions (e.g., *imi1::kanMX6*, *imi1Δ*). The deletion of *IMI1* is as follows: *IMI1*(30, 2812)::*kanMX6*, which means that the *IMI1* open reading frame has been replaced by *kanMX6*, a kanamycin resistance gene conferring G418 resistance on *S. cerevisiae*. The open reading frame is deleted from nucleotide 30 through 2812, where 30 is the A 30 nucleotides downstream from the ATG START codon and 2812 is the T immediately following the STOP codon. The *kanMX6* cassette was PCR-amplified from plasmid pFA6a- *kanMX6* (Bähler *et al*., 1998) using primers 5'GACGAAAGCGTTGCTATCAATGGTTGTCCAAATTTGGATTTCAACTGGCACGCC AGATCTGTTTAGCTTGCC3' and 5'GGTTTATATGGTATACGAACGAGAATGGCGTAGGGACATGAAAGATGGTAGAA TGGTTTAAACTGGATGGCGGCGTTAGTATC3'. The PCR product was transformed into W303 strain. The *IMI1* disruption was verified by PCR, genetic analysis and Southern blotting. Protein denoting is as follows: Imi1 encoded by *IMI1* gene. *S. cerevisiae* strains used in this study are listed in Table 1. Yeast culture media were prepared as described (Rose *et al*., 1990). YPD contained 1% Bacto-yeast extract, 2% Bacto-peptone and 2% (all w/v) glucose, YPGal as YPD but 2% galactose instead of glucose. SD contained 0.67% yeast nitrogen base without amino acids (Difco) and 2% glucose. For auxotrophic strains, the media contained appropriate supplements. Respiratory capacity was assessed on YPG medium (as YPD except glucose was replaced with 2% glycerol). For drop tests, cells were grown overnight in YPD or minimal media and adjusted to a density of OD_{600}=1. Growth was analyzed by plating 5-µL drops of 10-fold serial dilutions of cell suspensions onto solid media. Tests were repeated at

least three times. Standard methods were used for genetic manipulation of yeast (Rose *et al*., 1990). Plasmid propagation was performed in chemically competent *Escherichia coli* XL1-Blue MRF' (Stratagene).

Cadmium-induced formation of *petite* mutants

The assay is based on the fact that growth of yeast on glycerol-containing media requires mitochondrial respiration, while growth on glucose-containing media is possible without it (Shadel, 1999). Moreover, W303 strain and its derivatives bear *ade2-1* mutation which causes accumulation of an adenine-intermediate-derived pigment inside the vacuole that gives a red color to the colonies grown on medium containing limiting amounts of adenine (Sharma *et al*., 2003). However, respiratory-deficient cells lose this coloration and become white. To determine the rate of formation of cadmium-induced *petite* mutants the *imi1Δ* [rho^+(W303)] strain was constructed by back-crossing *imi1Δ* with W303 parental strain. Cells were grown o/n in liquid YPG medium to stationary phase and were then diluted in SD medium (with appropriate nutritional supplements) to OD_{600}=0.05. Where indicated, SD medium was supplemented with 20 μM $CdCl_2$. Samples were taken from the cultures after 20 h of growth at 30°C with shaking (200 rpm) on a rotary shaker, diluted to ca. 100 CFU per plate, plated on YPD medium and grown for 7 days at 30°C. The number and color of colonies was determined and the percentage of white colonies was calculated. Respiratory competence of randomly picked white and red colonies was verified on YPG medium. At least 15 red and 15 white colonies counted in each experimental condition in each repetiton were tested. As expected, all red colonies were respiration-competent and all white ones were respiration-incompetent (*petite*). The experiment was repeated three times.

Plasmid construction

IMI1 open reading frame together with flanking regions of ca. 850 bp at either side was PCR-amplified from genomic DNA of W303 wild-type strain using TaKaRa LA Taq polymerase (Takara Bio, Inc) and primers 5P037cF (5'CTGTACAAGACCGAGTGTTCGTTC3') and 3P039cR (5'GCATTAGCCACGTAGGAAGCAG3'). The amplified DNA (4445 bp) was cloned into pGEM-TEasy vector (Promega) and sequenced. The resulting plasmid pGEM-*IMI1* was used as a basis for subsequent constructs which are listed in Table 2. The nucleotide sequence of *IMI1* has been deposited in GenBank (KC256787.1). The Imi1-RFP fusion protein was constructed by PCR amplification of Imi1-encoding sequence together with upstream region, from nucleotide -850 to 2808, where 1 represents A of ATG START codon and 2808 is the last nucleotide (T) before the STOP codon. Primers used: 5P037cF (5'CTGTACAAGACCGAGTGTTCGTTC3') and IMI1-SalI (5'GCCGTCGACAATGAAAGCTAGAGGAAGAGCGG3'). After the T the GTCGAC sequence was introduced bearing SalI-recognition site, which enabled further gene fusion. SalI-digested PCR product was cloned into SalI-EcoICRI digested pUG35 plasmid in which GFP-encoding sequence was replaced by RFP-encoding gene PCR-amplified from pDB790 plasmid (Campbell et al., 2002; Balciuniene *et al*., 2013). The final plasmid was named P_{IMI}-*IMI-RFP*. The plasmid P_{tetO}-*IMI1-RFP* was constructed by PCR amplification of the whole Imi1-RFP-encoding sequence using P_{IMI}-*IMI-RFP* as template and primers 5'ATGGTTGTCCAAATTTGGATTTCAAC3' and 5'TTAGGCGCCGGTGGAGTGGCGGCC3' and cloning of the blunt-ended product into HpaI-digested pCM189 vector (Gari *et al*., 1997). The plasmid P_{tetO}-*IMI1* was constructed by cloning PCR-amplified *IMI1* to pCM189 vector using pGEM-*IMI1* as a template and 5'ATGGTTGTCCAAATTTGGATTTCAAC3' and 5'CTAAATGAAAGCTAGAGGAAGAG3' primers. All plasmids were verified by restriction analyses and DNA sequencing.

160
161
162 **mtDNA isolation and restriction enzyme digestion**
163 mtDNA was obtained from isolated mitochondria (Defontaine et al., 1991). Briefly, an
164 overnight 20-mL culture grown in YPD at 28°C under shaking was harvested by
165 centrifugation at 500 x g for 5 min. The pellet, 0.3 - 0.4 g wet weight, was washed twice in
166 water and once in 1.2 M sorbitol, 50 mM EDTA, 2% mercaptoethanol, resuspended in 5 mL
167 of 0.5 M sorbitol, 10 mM EDTA, 50 mM Tris, pH 7.5 containing 2% mercaptoethanol and 1
168 mg/mL of Zymolyase 100 T, and then incubated at 37°C for 45 min. Subsequent steps were
169 carried out at 4°C. The suspension was sonicated 3 x 1 min in a Bioruptor UCD-200
170 (Diagenode) set at H-level and the lysate was centrifuged at 3000 x g for 10 min. The
171 supernatant containing mitochondria was centrifuged at 15000 x g for 15 min, and the crude
172 mitochondrial pellet was collected and then rinsed four times with the same solution lacking
173 Zymolyase to eliminate genomic DNA contamination. The mitochondria were resuspended in
174 0.2 mL of 100 mM NaCl, 10 mM EDTA, 1% Sarcosyl, 50 mM Tris, pH 7.8 and allowed to
175 lyse for 30 min at room temperature. The mitochondrial lysate was extracted with phenol-
176 chloroform and nucleic acids were precipitated with 2 vols of ethanol from the aqueous phase.
177 The pellet was dissolved in water, digested with RNAse A for 30 min at 37°C, and purified
178 again by phenol-chloroform extraction and ethanol precipitation. The obtained mtDNA was
179 digested with restriction enzymes using buffers and digestion conditions provided by the
180 enzymes' manufacturers, electrophoresed in 0.5% agarose in TBE, stained with ethidium
181 bromide and photographed under UV illumination.
182
183 **Western blotting**
184 To visualize RFP-tagged proteins on Western blots, protein samples (100 μg $lane^{-1}$) were
185 subjected to 10% SDS–PAGE in Laemmli system (1970), at 10 V cm^{-1}, usually for 1.5 h,

followed by wet blotting onto Hybond-C extra membrane (in 25 mM Tris pH 8.3, 192 mM glycine and 20% methanol) and probing with an anti-RFP antibody (Living colors DsRed Polyclonal antibody, Clontech, Cat. No. 632496) diluted 1000-fold. Secondary anti-rabbit, alkaline phosphatase-conjugated antibodies (Promega, Cat. No. S3731) diluted 1:7500 and Western Blue Stabilized Substrate for Alkaline Phosphatase (Promega, Cat. No. S3841) were used to detect proteins.

Fluorescence microscopy

To visualize RFP-tagged Imi1 a Carl Zeiss AxioImager M2 fluorescence microscope (MicroImaging GmbH) with a 100x objective was used. RFP fluorescence was observed using a 20 HE filter set (Carl Zeiss, Cat. No. 489020-0000-000). Images were captured using an AxioCam MRc 5 camera (Carl Zeiss). DNA was stained with DAPI (4',6-diamidino-2-phenylindole) by incubating cells in fresh growth medium supplemented with 2.5 μg mL^{-1} of DAPI for 1 h at 30 ^{o}C.

Electron microscopy

For electron microscopy cells were fixed in 1.5% paraformaldehyde and 3% glutaraldehyde in 0.1 M sodium cacodylate buffer (pH 7.4) for 2 h at 4^{o}C. Cells were washed with the same buffer and post-fixed with 6% $KMnO_4$ in 0.1 M cacodylate buffer for 1 h, then washed in 30% ethanol and further dehydrated in a graded ethanol series, and embedded in Epon 812. Ultrathin sections were mounted on copper grids and air-dried. The sections were examined and photographed with a JEOL JEM 1011 electron microscope (Jeol, Tokyo, Japan).

Glutathione determination

For glutathione quantification yeast were grown overnight in SD medium with necessary auxotrophic supplements and 1.5-mL samples of the cultures were spun down in a microfuge at 14 000 rpm for 5 min. To determine intracellular oxidized glutathione (GSSG) cells were extracted with 12% perchloric acid with 50 mM NEM (*N*-ethylmaleimide). The excess of NEM was removed by hexane extraction and GSSG was determined fluorimetrically with glutathione reductase (Bergmeyer, 1983, Winiarska *et al*., 2003). Reduced glutathione (GSH) was determined by a modification of the method of Hiraku *et al.* (2002). For intracellular GSH measurements cells were extracted with 12% perchloric acid with 0.4 mM $Na_2S_2O_5$. To measure GSH in growth medium 500 µL of culture supernatant after sedimenting cells was mixed with equal volume of 24% perchloric acid with 0.8 mM $Na_2S_2O_5$. Samples were separated on an Agilent Zorbax SB-C18 reversed-phase column (5 µm, 4.6 x 250 mm) at a flow rate of 1 mL min^{-1} and column temperature of 30°C using a Dionex ICS3000 HPLC apparatus (Thermo Scientific, Waltham, USA) with electrochemical detector. The mobile phase contained 99 mM phosphate buffer (pH 2.5), 1% methanol (v/v), 200 mg L^{-1} sodium-1-octanesulfonate and 5 mg L^{-1} EDTA. The gold electrode potential was set at +0.78 V against an Ag/AgCl reference electrode. The amounts of GSSG and GSH are expressed as µmol g^{-1} dry weight of cells used for extraction or of cells sedimented from medium used for determination.

Phytochelatin determination

Phytochelatins (PCs) were determined according to the procedure of Wojas *et al*. (2008) adapted for yeast. A total of 75 OD_{600} units of yeast culture was spun down and cells were homogenized (3 x 50 s, 6500 rpm) with glass beads using MagNALyser (Roche) in 1 mL of a mixture composed of 890 µL of 6.3 mM diethylenetriaminepentaacetic acid, 50 µL of 1 M NaOH, 50 µL of 6 M $NaBH_4$ (in 0.1 M NaOH), and 10 µL of 1 mM *N*-acetyl-L-Cys (an

internal standard). The whole procedure was conducted at 4°C and samples and all solutions were kept on ice. The homogenate was centrifuged in a microfuge (10 min, 14 000 rpm) and 250 µL of the obtained extract was mixed with 10 µL of 20 mM monobromobimane and 450 µL of 4-(2-hydroxyethyl)-1-piperazine-3-propane sulfonic acid (HEPPS) buffer (pH 8.2) containing 6.3 mM diethylenetriaminepentaacetic acid. Derivatization was performed at 45°C in the dark for 30 min and stopped with 300 µL of 1 M methanesulfonic acid. The reaction mixture was filtered through 0.22-µm filter and stored at 4°C in the dark until HPLC analysis. Non-protein thiols were separated using a Waters 2695 HPLC apparatus (Waters Alliance, USA) with a Waters 2997 PDA detector and Nova-Pak C18 (Waters) column. Separation was carried out at 37°C using a methanol-water gradient, both with 0.1% trifluoroacetic acid. The injection volume was 20 µL. GSH and phytochelatin-2 (PC-2) (ANAWA Trading, # 60791) were used for column calibration. The data were integrated using Waters Millenium software.

Protein determination

Cell extract prepared for phytochelatin quantification was mixed with 4 volumes of ice-cold acetone and centrifuged for 10 min at 14 000 rpm, the pellet was rinsed with 80% acetone, air-dried and dissolved in 6 M urea. Protein was determined by the method of Bradford (1976).

***In silico* analyses of amino acid sequences**

Amino acid sequences were analysed using The Basic Local Alignment Search Tool (BLAST) tools (Acland *et al*., 2014). Repeats in Imi1 protein were identified using the TRUST program (Szklarczyk & Heringa, 2004). Proteins with repeated motifs were found using the Pattern Search program available on the http://myhits.isb-sib.ch website (Pagni *et al*., 2007). The indicated sequence source was UniRef50 and no taxonomic restriction was

applied. Full sequences of the identified proteins were obtained from the UniProt KB database (UniProt Consortium, Apweiler *et al*., 2014) and domains were identified in those sequences using Pfam (Finn *et al*., 2014) and HHpred (Hildebrand *et al*., 2009). The MAFFT alignment was then analysed using protein PSI-BLAST (Altschul & Koonin, 1998) algorithm to identify other similar repeats that were missed by Pattern Search. Their domains were identified using Pfam (Finn *et al*., 2014) and HHpred (Hildebrand *et al*., 2009), similarly as in the first set of proteins found. Solenoid structure was analyzed using REPETITA server (http://protein.bio.unipd.it/repetita/) (Marsella *et al*., 2009). Secondary structures were analysed using Quick2D server (http://toolkit.lmb.uni-muenchen.de/quick2_d/).

Results

Imi1-encoding DNA sequence has diverse organization in two popular yeast strains

The Imi1 (Irr1-mediated-interaction) protein was discovered in a two-hybrid screen (manuscript in preparation) for interactors of the Irr1/Scc3 protein, primarily involved in chromosome segregation (Kurlandzka *et al*., 1995; Toth *et al*., 1999). Basing on the data from the *Saccharomyces* Genome Database (SGD) we initially identified the prey protein as Prm7 encoded by the *YDL039C* ORF of a poorly defined function. Since the SGD genomic sequence represents the reference strain S288c (Mortimer & Johnston, 1986) and we were using another popular laboratory strain, W303 (Thomas & Rothstein, 1989), showing substantial genomic divergence from S288c (Ralser *et al*., 2012), we sequenced the relevant region in W303 DNA. The sequence obtained was clearly different from the S288c one: in addition to several small deletions and point mutations the two sequences had a different functional organization. In S288c the 2097 nucleotide-long ORF *YDL039C* (*PRM7*) is preceded by *YDL037C* (*BSC1*) of 986 nucleotides, terminating with a single STOP codon and followed by 519 nucleotides of an intergenic, apparently non-coding region. In W303 that

STOP codon is absent and as a consequence a continuous ORF comprising *YDL037C*, *YDL039C* and the intergenic region (together, 2811 bp) is formed, encoding a putative protein of 936 amino acids. The reading frame is preserved so its amino acid sequence is largely identical with the two shorter ones encoded in the S288c genome, apart from the "linker" corresponding to the stretch separating the two ORFs of S288c. Fig. 1. shows the organization of the genomic region in question in the two strains.

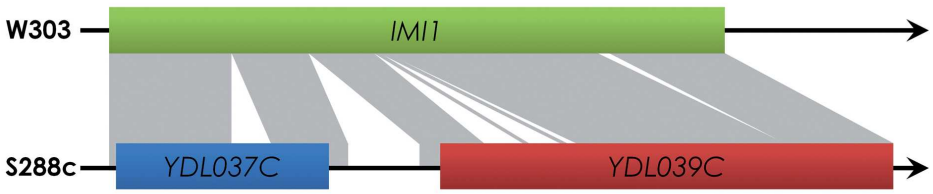

Fig. 1

Fig. 1. *S. cerevisiae* chromosome IV region encompassing *IMI1* in W303 and ORFs *YDL037C* and *YDL039C* in S288c strain.

To see which organization is predominant among diverse yeast strains, we examined the nucleotide seqences of the region corresponding to *IMI1* in 17 other *S. cerevisiae* strains whose genomes were available in databases and sequenced this region in four wine strains commercially available in Poland. Strains SK1, Y55, DBVPG6044 and three Polish wine strains contain one continous ORF, almost identical with *IMI1*, wherease in 15 strains two separate ORFs are present. The length of *YDL039C* ORF varies from 1542 to 3795 bp, and that of *YDL037C* from 834 to 1114 bp (data not shown).

Imi1 protein has a repetitive structure

To infer the cellular function of Imi1 we performed diverse bioinformatic analyses of its amino acid sequence and putative structure. We found that its N-terminal part (amino acids 1-

153) is likely to form a Flo11 domain (Pfam: PF10182, HHpred similarity analysis: probability: 100, e-value: 9e-58). This domain has been identified in 65 proteins of *Ascomycota* (http://smart.embl-heidelberg.de), most of which are only putative and uncharacterized. For some, an involvement in flocculation and pseudohyphal growth is deduced basing on an analysis of respective null mutants. No direct characteristics of any of those proteins could be found.

Since we could not deduce an Imi1 function basing on its similarity to known proteins, we analysed its architecture. We noticed that outside the N-terminal Flo11 domain Imi1 contains numerous repeated regions of different lengths. We identified a previously unknown sequence motif [TS]-[SP]-X-D-P-[TS]-[TS]-S-[VIST]-X-[TSIV]-[ST], containing numerous serine and threonine residues. In positions 4-7 of the motif aspartic acid – proline – threonine - serine is usually present, therefore we named the whole 12-amino acid repeat the DPTS motif.

In all, Imi1 contains seven perfect and at least nine imperfect DPTS motifs scattered throughout its C-terminal part but mostly concentrated in its central region (Fig. 2). In addition to Imi1, numerous other, mostly yeast, proteins containing the DPTS motif were found in databases, representing several types of overall domain architecture, as shown in Fig. 3.

Fig.2

Fig. 2. Distribution of DPTS repeats in Imi1 amino acid sequence. The N-terminal part of Imi1 (boxed) is the Flo11-like domain. The remaining part contains perfect (red) and imperfect (blue) DPTS motifs.

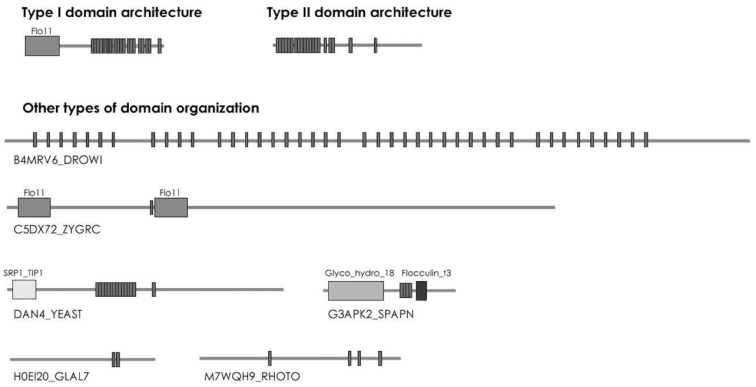

Fig. 3

Fig. 3. Domain organization of DPTS repeat-containing proteins. Types I and II are similar to whole Imi1 and its C-terminal part, respectively. Narrow unmarked bars depict DPTS motifs, larger boxes represent indicated domains.

An independent bioinformatic and experimental analysis of the region encompassing *YDL037C-YDL039C* in S288c has been performed earlier by Namy *et al*. (2003). They found that in S288c the STOP codon of *YDL037C* can be bypassed with 25% efficiency. Four amino acid repeats (TTSVDPTTS), spaced by 15 amino acids, around the *YDL037C* STOP codon and in the intergenic region were shown to be critical for the STOP codon read-through.

Using the REPETITA server (Marsella *et al*., 2009) we found that, except for its N-terminal Flo11 domain, Imi1 forms a solenoid. Solenoids are modular assemblies of structurally identical units. They contain secondary structure elements, β-strands or α-helices, coiled along a common axis and with a fixed curvature (Marsella *et al*., 2009).

The prediction of solenoid-forming repeats in Imi1 is highly significant (z_{max} = 9 and ρ_θ = 4.6, where z_{max} is the significance of the detected periodicity in the sequence under analysis and ρ_θ represents the deviation from an experimentally set threshold) (Fig. 4). These results

strongly indicate that the DPTS repeats in Imi1 form a characteristic periodic winding structure. According to a Quick2D server prediction the solenoid is predominantly composed of α-helices with the repeat length of 12 amino acids.

Thus, while indicating a very interesting novel motif for Imi1 and a few structurally related proteins, the modeling offered little clue as to the possible functions of Imi1.

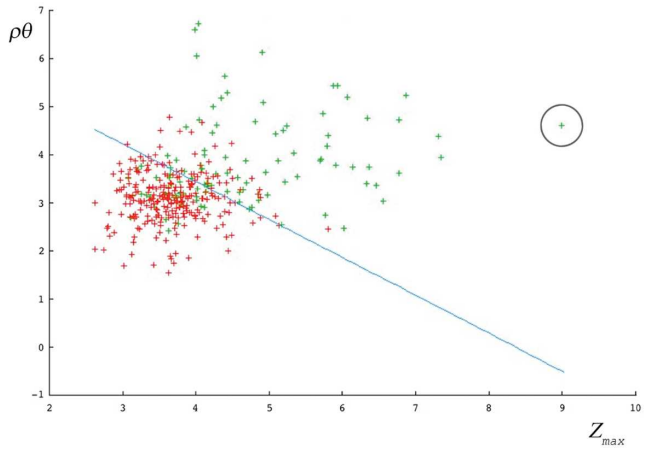

Fig. 4

Fig. 4. The C-terminal part of Imi1 likely has a distinct solenoid structure. The Imi1 amino acid sequence without the N-terminal part (amino acids 1-153, including the Flo11 domain) was analyzed using the REPETITA server and the z_{max} and ρ_θ values obtained were plotted together with those for a benchmark set of proteins of known structure (red, non-solenoids, green, solenoids). The line represents best separation between solenoid and non-solenoid structures. Encircled is position of Imi1.

Database analysis suggests promiscuous action of Imi1

To predict the role(s) played by Imi1 we turned to databases reporting results of large-scale studies on physical and genetic interactions. Unfortunately, since the studies reported have been carried out in the background of the S288c strain, no direct reference to Imi1 or its gene could be found. Data from genome-wide protein-protein interactions (Tarassov *et al*., 2008) and a proteome chip study of protein phosphorylation (Ptacek *et al*., 2005) reporting the

two putative proteins encoded by *YDL037C* and *YDL039C*, corresponding to the N- and C-terminal parts of Imi1, were not very conclusive. They have revealed that the *YDL037C*-encoded protein Bsc1 interacts with Rtc1, a subunit of the SEA complex engaged in intracellular vesicular transport, and the Prm7 protein encoded by *YDL039C* interacts with protein kinases Hal5, Hek2, Kin82, Prr2, and Yck2, and with the Nam7 protein involved in nonsense-mediated mRNA decay.

All the genetic interactions of *YDL037C* and *YDL039C* were identified in a genome-scale genetic interaction screen looking for a significant deviation of the fitness of a double mutant compared with the expected multiplicative effect of the two respective single mutants (Costanzo *et al*., 2010). For *YDL037C* two such interactions, with *SMT3* and *STR2*, have been found. *SMT3* encodes SUMO, a small protein similar to ubiquitin, whose post-translational atachement to other proteins modulates their functioning. The second gene, *STR2*, encodes cystathionine γ-synthase. This enzyme converts cysteine to cystathionine and thus, by consuming cysteine, modulates GSH level. In *str2Δ* strain an excess of GSH is produced but is degraded by specific peptidases (Ganguli *et al*., 2007), whereas overexpression of *STR2* decreases the intracellular glutathione concentration (Suzuki *et al*., 2011). The *str2Δydl037cΔ* strain grows slower than could be expected from the effects of the single deletions (Costanzo *et al*., 2010), suggesting that the *YDL037C*-encoded protein could be involved in the metabolism of sulfur amino acids.

Many more genetic interactions (45) have been reported for ORF *YDL039C*, corresponding to the 3'-part of *IMI1* gene and encoding most of the predicted solenoid domain of Imi1. Among these genetic interactors the largest group (12) comprises genes related to mitochondria (*AIM36*, *ATP23*, *CMC1*, *ERT1*, *GCV2*, *MDL1*, *MDM12*, *PET20*, *PUF3*, *RML2*, *UPS1*, *YBR238C*, *YHM2*). This suggests a likely involvement of the *YDL039C*-encoded protein, and by inference also of Imi1, in mitochondrial processes. Other interactions

393 are rather diverse and include genes related to RNA metabolism (8 genes), transcription (5),
394 protein kinases (*ERG8*, *RIM15*, *TPK3*) possibly phosphorylating the protein, and various
395 metabolic processes.
396 Also genome-wide deletion analyses in yeast missed the *IMI1* gene and only reported
397 phenotypes of the *ydl037c*Δ and *ydl039c*Δ strains. The phenotypes of *ydl037c*Δ included an
398 increased competitive fitness regardless of carbon source in growth medium, and increased
399 sensitivity to cycloheximide, methylglyoxal, and streptomycin. For *ydl039c*Δ strain some
400 analyses indicated an increased competitive fitness upon growth on glycerol- or ethanol-
401 containing medium, but others actually reported a lack of respiratory growth and increased
402 mitophagy and glutathione excretion.
403
404 **Deletion of *IMI1* causes rearrangements of mitochondrial DNA and alters mitochondrial**
405 **morphology**
406 The Imi1 structure modeling and the analysis of reported data on the two shorter ORFs
407 did not indicate unequivocally a role Imi1 could play in the cell, but suggested several
408 processes in which the protein was likely involved. In the following experimental study of
409 Imi1 functions we focused on mitochondria and some aspects of sulfur amino acid
410 metabolism. We first checked whether the *IMI1* gene was required for cell viability, the Imi1
411 protein expressed, and where it localized. An *imi1Δ* mutant was constructed by replacing the
412 *IMI1* ORF with the kanamycin resistance gene *kanMX6.*
413 When analyzed on complete YPD medium the mutant was fully viable. However, it did not
414 grow on media containing ethanol, lactate or glycerol as a carbon source (see Fig. 5), which
415 indicated a likely respiratory incompetence. To verify this *imi1Δ* was crossed with a rho^0
416 tester strain MR6/b-3, a derivative of W303 (Godard *et al*., 2011). MR6/b-3 bears a wild copy
417 of *IMI1* but lacks the entire mitochondrial genome, thus the diploid's mitochondrial DNA

could only be derived from the *imi1*Δ strain while a functional Imi1 protein would be provided by the intact *IMI1* gene. The obtained *imi1*Δ/*IMI1*[*rho*^{0}] diploid did not grow on non-fermentable media (Fig. 5), which confirmed the lack of respiration-competent mitochondria in *imi1Δ* cells.

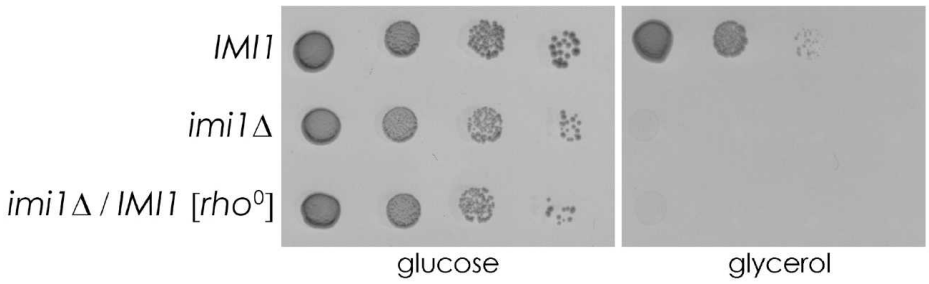

Fig. 5

Fig. 5. Deletion of *IMI1* gene precludes mitochondrial respiration. Indicated strains were grown in YPD medium and diluted to identical concentrations. Serial 10-fold dilutions were spotted onto YPD (containing 2% glucose, left) and YPG (containing 2% glycerol, right) and incubated at 30°C for two days.

To characterize further the mitochondrial dysfunction of *imi1Δ* its mtDNA was isolated and subjected to restriction enzyme digestion, which demonstrated substantial rearrangements of the mtDNA compared to that of the parental *IMI1* strain (Fig. 6). Notably, those rearrangements differed between individual *imi1Δ* clones.

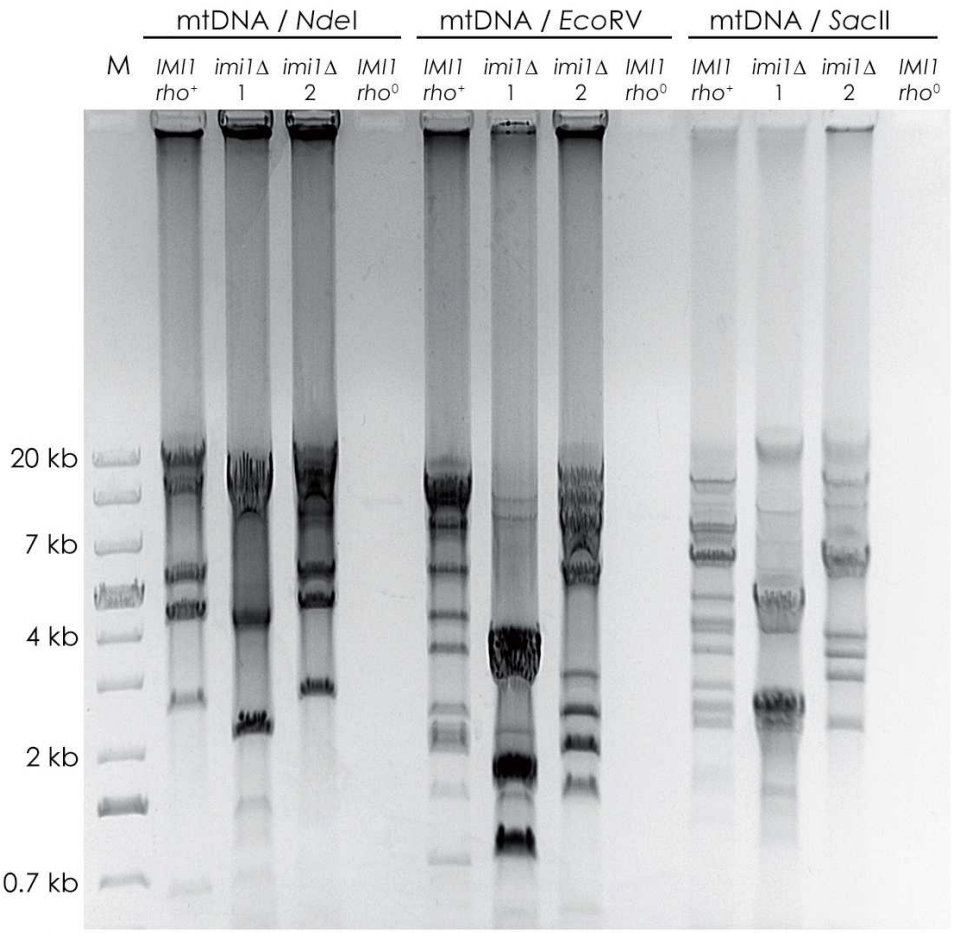

435 Fig.6

436 **Fig 6.** mtDNA is rearranged in *imi1Δ*. Negative image of ethidium bromide-stained agarose
437 gel after electrophoresis of NdeI, EcoRV or SacII-digested mtDNA of parental *IMI1* strain
438 and two *imi1Δ* clones (1, 2). *IMI1*[*rho*^{0}] – control MR6/b-3 strain, devoid of mtDNA, M –
439 DNA size marker.
440

441 We then studied mitochondrial morphology of *imi1Δ* cells using transmission electron
442 microscopy. As shown in Fig. 7, in *imi1Δ* mitochondria the cristae are reduced or absent.
443 Thus, a lack of Imi1 leads to mtDNA instability and to major defects of the mitochondrial
444 inner membrane.

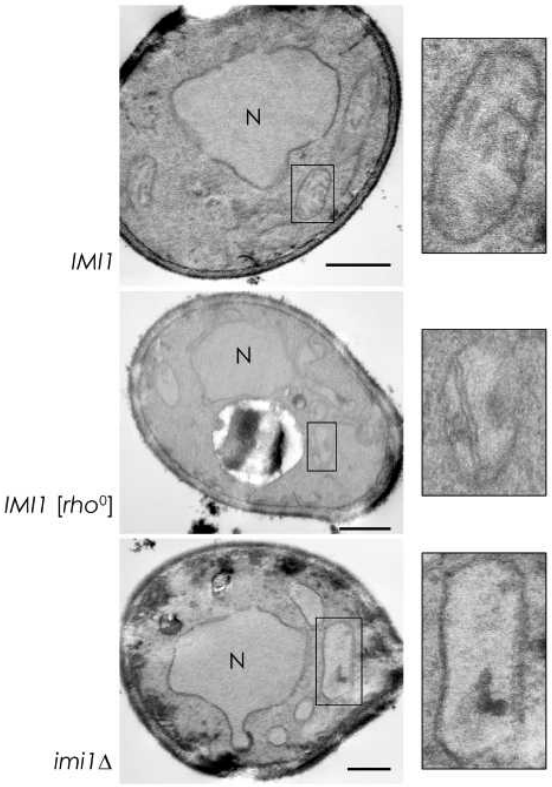

Fig. 7

Fig. 7. Deletion of *IMI1* gene affects mitochondrial morphology. Transmission electron micrographs of cells of *IMI1* (wild type), *IMI1*[*rho*^{0}] (as *IMI1* but devoid of mtDNA), and *imi1Δ* mutant strain. Mitochondrial structures typical for a given strain are shown on the right. N – nucleus. Bar, 500 nm.

Imi1 is likely localized in the cytoplasm

The experiments described above showed that deletion of *IMI1* gene affected cell functioning, suggesting that the gene encodes a functional p

rotein. To confirm this conclusion and to establish the cellular localization of the *IMI1*-encoded protein we constructed two *IMI1-RFP* fusion genes, one controlled by the original *IMI1* promoter (P_{IMI1}) and the second – by the tetracycline-regulatable *tetO* promoter (P_{tetO}) (Gari *et al*., 1997). Either gene was introduced on a centromeric plasmid (see Table 2) to the *imi1Δ* mutant. To confirm correct expression of the chimeric protein, Western blotting of whole-cell extracts was performed. Upon expression of *IMI1-RFP* from the original promoter the protein was undetectable but the construct driven by the strong *tetO* promoter produced

enough protein to allow its detection (Fig. 8a). The electrophoretic mobility of the anti-RFP reactive band was substantially less than expected from the calculated molecular mass of Imi1-RFP (122 kDa), albeit one should note that the resolution of the gel in the high-molecular-mass region is too low for exact mass determination. It is also likely that owing to its peculiar structure the protein migrates aberrantly.

To localize Imi1-RFP in the cells they were subjected to fluorescence microscopy. Consistent with the Western blotting results, expression of *IMI1-RFP* from the original promoter did not produce a detectable signal (Fig. 8b), while in cells expressing P_{tetO}-*IMI1-RFP* the red signal was clearly visible and was predominantly present in the cytoplasm (Fig. 8C), without any accumulation in the vacuole or the nucleus. These data show that under standard conditions Imi1 is a low-abundance protein. When overexpressed, it is not degraded nor forms aggregates, but it cannot be excluded that its predominant uniform cytoplasmic localization masks faint signals from organelles or membrane structures.

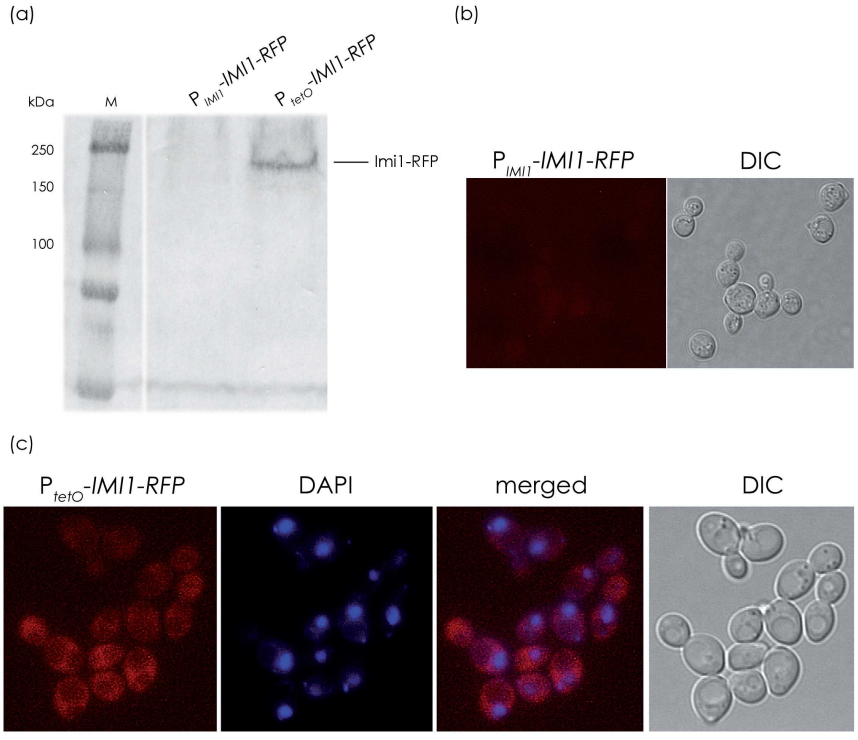

Fig.8

Fig. 8. *IMI1* encodes a low-abundance protein which, when overexpressed, is predominantly localized to cytoplasm. (a) Immunoblot of soluble protein extract of whole cells bearing *IMI1-RFP* fusion gene under original P_{IMI1} or P_{tetO} promoter. Imi1-RFP fusion protein was detected using anti-RFP antibodies. (b) Imi1-RFP fluorescence is undetectable upon expression from the original P_{IMI1} promoter. (c) Upon expression from the P_{tetO} promoter Imi1-RFP fluorescence is present in cytoplasm. Cells of *imi1Δ* strain bearing respective plasmids encoding Imi1-RFP were grown in SD medium with appropriate supplements. Localization of Imi1-RFP was followed by direct RFP fluorescence. For visualization of DNA, cells were stained with 4,6-diamidino-2-phenylindole (DAPI), DIC - differential interference contrast.

Deletion of *IMI1* gene impairs GSH/GSSG balance

Since the major antioxidant protection mechanism involves glutathione, and mitochondria are the major source and also target of ROS, we reasoned that the observed mitochondrial defects could be associated with a disturbed glutathione homeostasis in *imi1Δ* cells. Also the database information discussed above suggested a connection of Imi1 with cysteine/glutathione metabolism. To verify this assumption we determined the level of reduced and oxidized glutathione. We found that the *imi1Δ* mutant contained ca. 40% less GSH than the parental *IMI1* strain (Fig. 9a). Notably, expression of *IMI1* from a plasmid only partially reverted the depletion of GSH. The level of intracellular GSSG was similar in the *IMI1* and *imi1Δ* strains (Fig. 9a). As a consequence, both the total content of glutathione and, more importantly, the GSH/GSSG ratio, were decreased in *imi1Δ* relative to the wild type. Those changes were not caused by excessive GSH secretion to the medium, as it was at a similar very low level in both strains (Fig. 9b). The level of GSSG in the growth medium was also fairly similar for the two strains (ca. 8±1.2 μmol g^{-1} d.w., not shown).

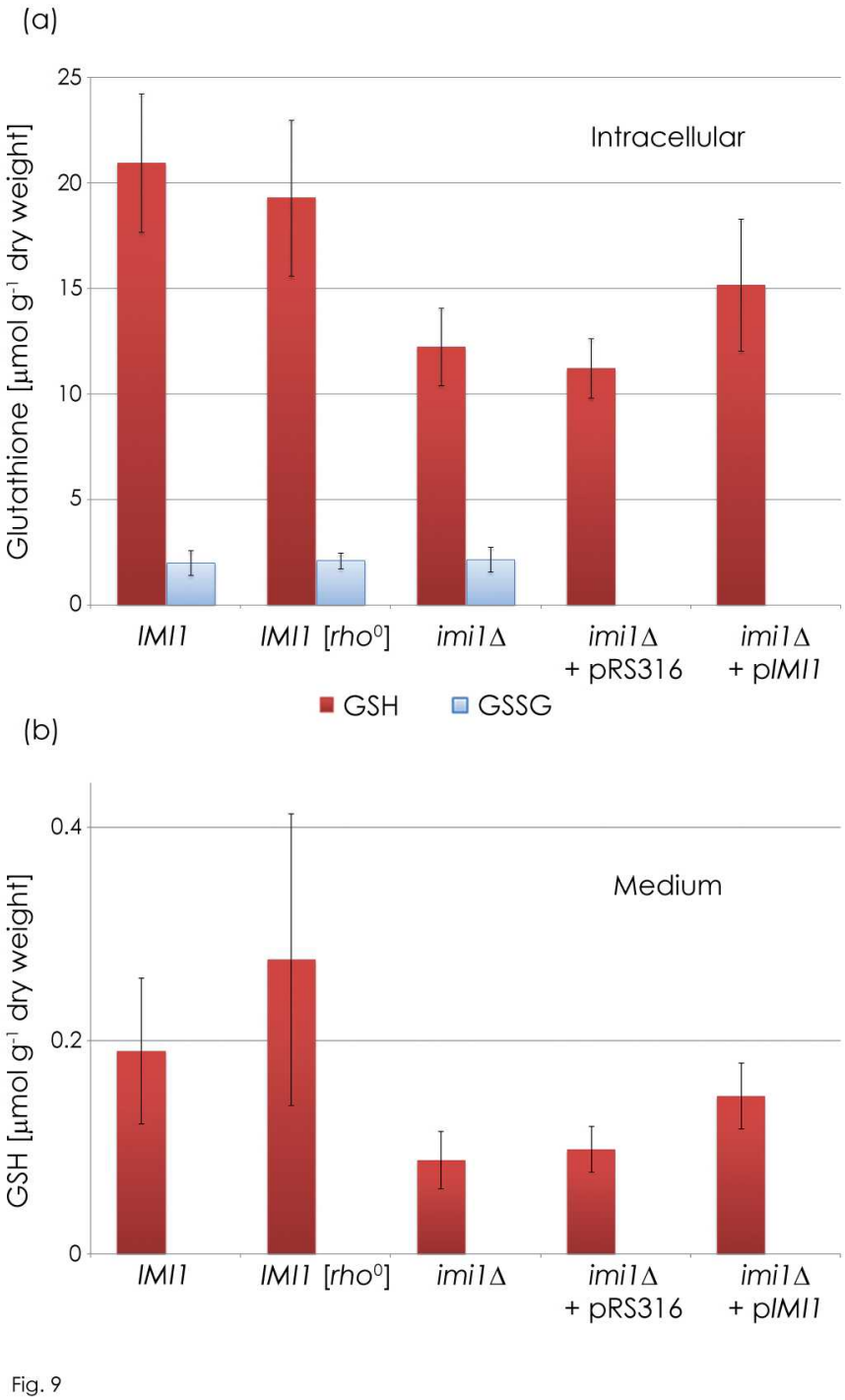

Fig. 9

Fig. 9. Deletion of *IMI1* gene decreases intracellular GSH content. (a) intracellular GSH and GSSG, (b) GSH in growth medium. Cells were grown o/n in YPD medium, diluted to OD_{600} = 0.05 in SD medium and grown for 20 h. The values are the mean ± SD of three independent experiments, each determined in triplicate.

506 Yeast strains with an altered glutathione redox state are hypersensitive to oxidative
507 stress induced by peroxides (Grant *et al*., 1998). We found that also the *imi1Δ* mutant showed
508 an increased sensitivity to oxidative agents present in growth medium (Fig. 10a). Introduction
509 of an *IMI1*-bearing plasmid (p*IMI1*) into *imi1Δ* suppressed this sensitivity only marginally
510 probably due to the damage of cellular structures accumulated in *imi1Δ* cells prior to their
511 transformation with p*IMI1*, and this result parallelled the incomplete restoration of GSH level
512 found earlier (Fig. 9). Overexperssion of *IMI1* from the strong P_{tetO} promoter actually
513 increased the sensitivity to H_2O_2 compared to *imi1Δ* (Fig 10a, bottom lane), which suggests
514 that a tightly controlled level of Imi1 is required for optimal cell defence against oxidizing
515 agents.
516 To verify whether the increased sensitivity of *imi1Δ* to oxidizing agents is caused by its
517 defective mitochondria, we constructed an *imi1Δ* [rho^+(W303)] strain by back-crossing with
518 *IMI1*[rho^+]. That strain had the same sensitivity to hydrogen peroxide and $KMnO_4$ as the wild
519 type (Fig. 10b), which indicated the causative role of the mitochondrial dysfunction in the
520 increased sensitivity of *imi1Δ* to oxidative stress.
521

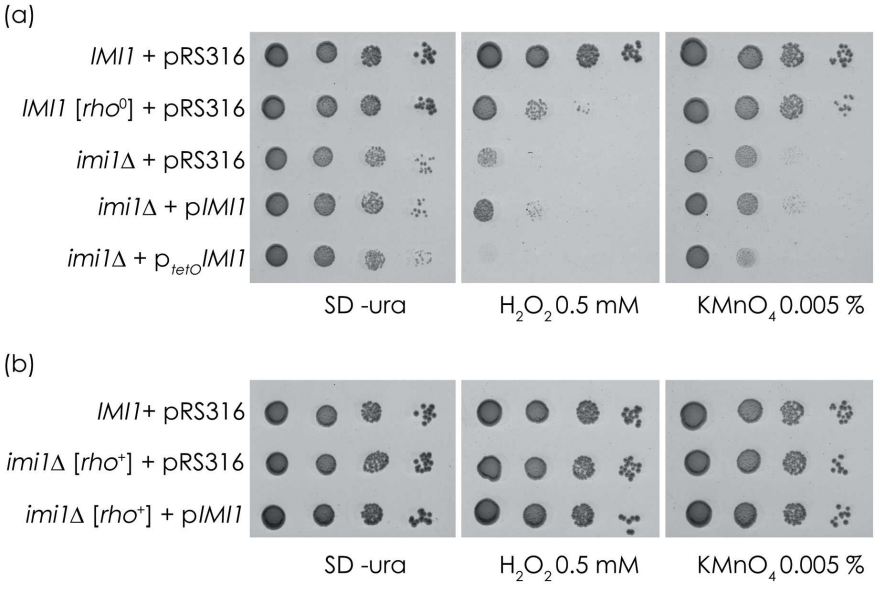

522 Fig.10.

Fig. 10. Deletion of *IMI1* gene increases sensitivity of yeast cells to oxidative agents likely due to mitochondrial damage. (a) *IMI1*, *IMI1*[rho^0] and *imi1Δ* strains bearing pRS316 plasmid or pRS316 with *IMI1* gene under original P_{IMI1} or P_{tetO} promoter. (b) *IMI1* and *imi1Δ* [rho^+] strains. Cells were grown in SD medium supplemented as appropriate and diluted to identical concentrations. Serial 10-fold dilutions were spotted onto SD medium and SD supplemented with 0.5 mM H_2O_2 or 0.005% $KMnO_4$. Cultures were grown at 30°C for two days.

Deletion of *IMI1* decreases cells sensitivity to cadmium likely due to increased level of phytochelatin-2

One of the functions of cysteine-containing peptides and proteins, such as metallothioneins, glutathione, or phytochelatins (PCs), is protection against the toxicity of heavy metals (Cobbett, 2000). Since *imi1Δ* cells had a lower content of glutathione, we checked their sensitivity to cadmium, expecting it to be enhanced. Surprisingly, the *imi1Δ* cells were less sensitive to cadmium than their *IMI1* counterparts (Fig. 11). The decreased cadmium sensitivity of *imi1Δ* was unlikely to be due to its mtDNA defects since *IMI1*[rho^0] was more cadmium-sensitive than *IMI1* (Fig. 11a). The increased cadmium-resistance of *imi1Δ* was not affected by introduction of intact mitochondria, but was abrogated by *IMI1* introduced on centromeric plasmid under original P_{IMI1} promoter. Overexperssion of *IMI1* from the strong P_{tetO} promoter did not influence the sensitivity of *imi1Δ* to cadmium compared to wild-type strain (Fig 11b, bottom lane).

To explain this conundrum we determined the level of PCs, which are synthesized from glutathione, in the *imi1Δ* mutant. *S.cerevisiae* has been reported to express exclusively phytochelatin-2 (PC-2) in limited amounts (Kneer *et al*., 1992; Wunschmann *et al*. 2007), and some studies even failed to detect any PC (Clemens *et al*., 1999). In agreement with the former, we detected PC-2 in both the control strain and the *imi1Δ* mutant (Fig. 11c). Notably, the *imi1Δ* mutant contained three times as much PC-2 as the wild type did (20.5 ± 6 pmol mg^{-1} protein vs. 7.5 ± 4 pmol mg^{-1} protein, average of two experiments). Cadmium exposure

did not affect those levels (not shown). Thus, the partial cadmium resistance of *imi1Δ* seems likely to be due to its elevated PC-2 level.

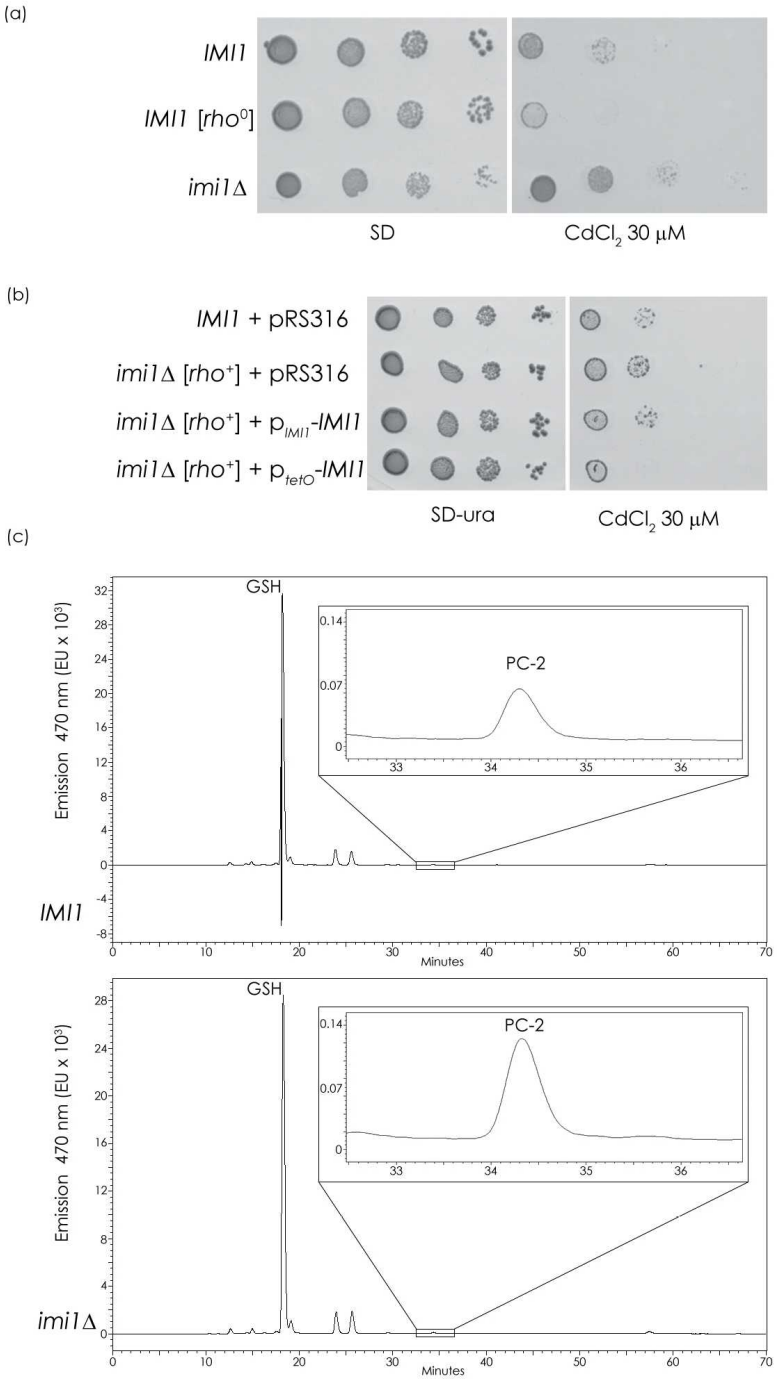

Fig. 11

Fig. 11. Deletion of *IMI1* gene decreases yeast sensitivity to cadmium likely due to increased PC-2 level. (a) *imi1Δ* strain is less sensitive to cadmium than *IMI1*, (b) *IMI1* reverts this partial resistance. Cells were grown in SD medium and diluted to identical concentrations. Serial 10-fold dilutions were spotted onto SD and SD + 30 μM $CdCl_2$. (c) HPLC analysis of cysteine-containing peptides from *IMI1* and *imi1Δ* strains. Peaks corresponding to PC-2 and GSH are marked. Extracts of *S. cerevisiae* cells were labeled with monobromobimane and analyzed by HPLC using a reversed-phase column and fluorescence detection. Two independent experiments were conducted giving highly similar results; one determination is shown.

To establish whether the decreased overall sensitivity of *imi1Δ* to cadmium was correlated with the protection of mitochondria against cadmium toxicity we performed a *petite*-mutant induction assay. Formation of *petite* mutants is a good measure of mtDNA integrity in yeast (Shadel, 1999). Since the original mitochondria of *imi1Δ* were strongly damaged, we used already mentioned *imi1Δ* [rho^+(W303)] strain and exposed it to 20 μM cadmium. This cadmium concentration did not significantly affect the cells (their viability was ca. 80%).

We found that *imi1Δ* [rho^+(W303)] produced ca. 50% less *petite* colonies than the wild-type *IMI1* did (Fig. 12). In the absence of cadmium the two strains showed the same rates of spontaneous *petite*-mutant formation. Thus, the *imi1Δ* mutation affords small, but significant protection of mtDNA against deleterious effects of cadmium.

The increased content of PC-2 in the *imi1Δ* mutant explained, at least in part, its decreased sensitivity to cadmium seen both as improved cell growth and decreased frequency of *petite* colonies. However, it could not explain the decreased GSH content of *imi1Δ* since PC-2 was present at a level much below 1% of GSH.

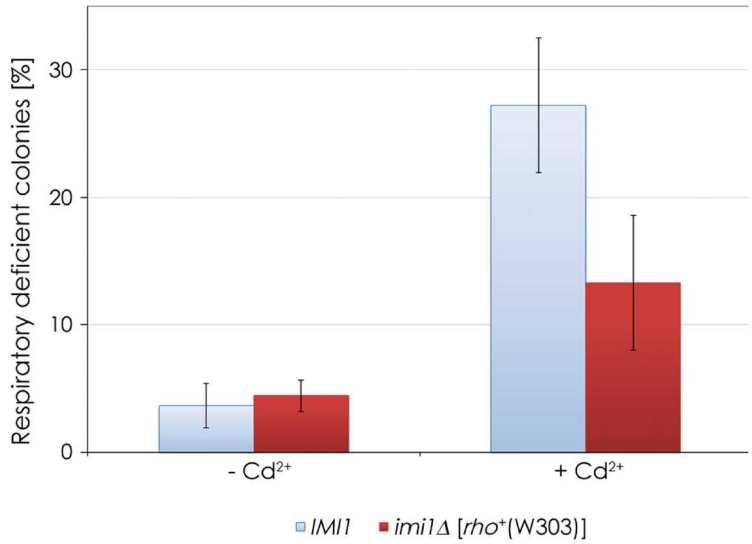

Fig. 12

Fig. 12. *imi1Δ* strain exhibits decreased frequency of cadmium-dependent *petite* formation. Yeast were grown o/n in YPG medium, diluted and grown for 20 h in SD medium supplemented or not with 20 μM $CdCl_2$, then plated on YPD medium and respiratory incompetent (white) colonies were scored after 10 days of incubation at 30°C. The values are the mean ±SD of three independent experiments.

Discussion

Much of our understanding of glutathione homeostasis at the molecular level is based on research done on *S. cerevisiae*. Here we describe a new low-abundance cytoplasmic protein Imi1 involved in this process. Imi1 seems specific to yeast and does not have homologues characterized at the molecular level. The Imi1 protein has not been reported before likely because in the reference yeast strain S288c the *IMI1* gene is split into two apparently independent ORFs. However, it has been found that in S288c the unique stop codon of *YDL037C* (*BSC1*), representing a part of *IMI1*, is bypasssed with 25% effciency (Namy *et al*., 2003). Thus, it is quite likely that a small amount of a read-through protein 84% identitcal with Imi1 is in fact present in S288c.

The intracellular glutathione level depends on its biosynthesis, degradation, and consumption in diverse processes, and additionally may be altered by its

compartmentalization and efflux from the cell (Perrone *et al*., 2005; Ganguli *et al*., 2007). A lack of Imi1 causes a 40% decrease of GSH level and thus a drop in the GSH/GSSG ratio. Since it has been demonstrated that as little as 1% of wild-type GSH level is sufficient to allow respiratory growth (Ayer *et al*., 2010), it is rather unlikely that the observed 40% decrease of its level destabilizes the mitochondrial genome and cristae. We propose instead that the lack of Imi1 causes a primary defect leading to mitochondrial damage. The resulting *petite* phenotype would cause an increased GSH utilization as a response to overproduction of ROS due to the malfunctioning of mitochondria.

Our data also indicate a role of Imi1 in the protection against heavy metal toxicity. Despite a decreased intracellular GSH content the lack of Imi1 actually improves the yeast tolerance of cadmium ions both at the general physiological level and at the level of mitochondrial genome stability. While the increased sensitivity to oxidizing agents is due to the *imi1Δ* cells being *petite*, the decreased cadmium sensitivity is independent of the mitochondrial defects. The protection of mitochondria against cadmium toxicity is likely linked to an increased production of phytochelatin-2.

The mechanism of cadmium toxicity is not fully understood although it has long been known that exposure to cadmium severely damages mitochondrial cristae (Lindegren & Lindegren, 1973; Thévenod, 2009). By increasing the production of mitochondrial ROS, cadmium causes mitochondrial membrane damage, mtDNA cleavage and impaired ATP generation (Tamas *et al*., 2006; Cuypers *et al*., 2010). Although cadmium has a high affinity for thiols and GSH is its primary target (Lopez *et al*., 2006), phytochelatins constitute an equally important chelating agent. It is believed that the presence of cadmium results in some GSH depletion affecting the redox balance and impairing the activities of GSH-dependent enzymes, thereby affecting diverse cellular processes (Wysocki & Tamas, 2010). Our results show that a low level of PC-2 can be detected in W303 strain without cadmium induction and

a lack of Imi1 increases this level three-fold. Therefore, *imi1Δ* is slightly more resistant to Cd^{2+} than the parental strain *IMI1*. Whether the increased PC-2 production in the absence of Imi1 is a consequence of the decreased GSH content and/or the GSH/GSSG ratio, or a direct effect of the lack of Imi1 remains to be established.

Finally, the *imi1Δ* yeast can be of practical interest as a convenient model of eukaryotic cell with a lowered glutathione content. Ample data indicate an association between suboptimal cellular glutathione levels and diverse diseases involving renal, hepatic, and especially brain tissue damage accompanied by mitochondrial dysfunction (Jain *et al*., 1991; Martensson *et al*., 1990; Wallace 2005; Wallace & Fan 2010; Lin & Beal, 2006; Calabrese *et al*., 2005). Notably, in Parkinson's disease GSH concentration is decreased by 30–40% in cells of substantia nigra pars compacta (Sofic et al., 1992; Sian et al., 1994), similarly as in the *imi1Δ* yeast cells. Thus, further studies of the *imi1Δ* defects and their molecular mechanism may help understand the causes and effects of altered glutathione homeostasis in disease.

Funding

This work was supported by the National Science Centre (NCN) [grant number UMO-2013/09/N/NZ3/00526].

The Dionex ICS3000 chromatograph used for glutathione determinations was supported by the Ministry of Science and Higher Education from the Funds of Science and Polish Technology [Decision 372/FNiTP/115/2009].

Acknowledgements

We thank Drs Jerzy Brzywczy, Aneta Kaniak-Golik and Róża Kucharczyk for advice and discussion and Dr. Michal Usarek for some HPLC determinations.

650 The authors have declared that no conflict of interests exist.
651
652 **References**
653 Acland A, Agarwala R, Barrett T, *et al*. (2014) Database resources of the National Center for
654 Biotechnology Information. *Nucleic Acids Res* **42:** D7-D17.
655
656 Altschul SF & Koonin EV (1998) Iterated profile searches with PSI-BLAST--a tool for
657 discovery in protein databases. *Trends Biochem Sci* **23:** 444-447.
658
659 Apweiler R, Bateman A, Martin MJ, *et al*. (2014) Activities at the Universal Protein Resource
660 (UniProt). *Nucleic Acids Res* **42:** D191-D198.
661
662 Ayer A, Tan SX, Grant CM, Meyer AJ, Dawes IW & Perrone GG (2010) The critical role of
663 glutathione in maintenance of the mitochondrial genome. *Free Radic Biol Med* **49:** 1956-
664 1968.
665
666 Ayer A, Gourlay CW& Dawes IW (2014) Cellular redox homeostasis, reactive oxygen
667 species and replicative ageing in *Saccharomyces cerevisiae*. *FEMS Yeast Res* **14:** 60-72.
668
669 Bachhawat AK, Ganguli D, Kaur J, Kasturia N, Thakur A, Kaur H, Kumar A & Yadav A
670 (2009) *Yeast Biotechnology: Diversity and Applications*, (Satyanarayana T & Kunze G, eds)
671 pp. 259-280. Springer, Netherlands.
672
673 Bähler J, Wu JQ, Longtine MS, Shah NG, McKenzie A 3rd, Steever AB, Wach A, Philippsen
674 P & Pringle JR (1998) Heterologous modules for efficient and versatile PCR-based gene
675 targeting in *Schizosaccharomyces pombe*. *Yeast* **14:** 943-951.

676 Balciuniene J, Nagelberg D, Walsh KT, Camerota D, Georlette D, Biemar F, Bellipanni G,
677 Balciunas D (2013) Efficient disruption of Zebrafish genes using a Gal4-containing gene trap.
678 *BMC Genomics* **14:** 619.
679
680 Bergmeyer HU (1983) *Methods in Enzymatic Analysis*. Verlag Chemie GmbH, Weinheim-
681 Basel.
682
683 Biegert A, Mayer C, Remmert M, Söding J & Lupas AN (2006) The MPI Bioinformatics
684 Toolkit for protein sequence analysis. *Nucleic Acids Res* **34:** W335-W339.
685
686 Bradford MM (1976) Rapid and sensitive method for the quantitation of microgram quantities
687 of protein utilizing the principle of protein-dye binding. *Anal Biochem* **72:** 248–254.
688
689 Burhans WC & Heintz NH (2009) The cell cycle is a redox cycle: linking phase-specific
690 targets to cell fate. *Free Radic Biol Med* **47:** 1282-1293.
691
692 Calabrese V; Lodi R; Tonon C; D'Agata V; Sapienza M; Scapagnini G; Mangiameli A;
693 Pennisi G; Stella AM & Butterfield DA (2005) Oxidative stress, mitochondrial dysfunction
694 and cellular stress response in Friedreich's ataxia. *J Neurol Sci* **233:** 45–162.
695
696 Campbell RE, Tour O, Palmer AE, Steinbach PA, Baird GS, Zacharias DA, Tsien RY (2002)
697 A monomeric red fluorescent protein. *Proc Natl Acad Sci U S A* **99:** 7877-7782.
698
699 Clemens S, Kim EJ, Neumann D & Schroeder JI (1999) Tolerance to toxic metals by a gene
700 family of phytochelatin synthases from plants and yeast. *EMBO J* **18:** 3325-3333.

Cobbett CS (2000) Phytochelatins and their roles in heavy metal detoxification. *Plant Physiol* **123:** 825–832.

Costa V, Quintanilha A & Moradas-Ferreira P (2007) Protein oxidation, repair mechanisms and proteolysis in *Saccharomyces cerevisiae. IUBMB Life* **59:** 293-298.

Costanzo M, Baryshnikova A, Bellay J *et al*. (2010) The Genetic Landscape of a Cell. *Science* **327**: 425-431.

Cuypers A, Plusquin M, Remans T *et al*. (2010) Cadmium stress: an oxidative challenge. *Biometals* **23:** 927-940.

Defontaine A, Lecocq FM & Hallet JN (1991) A rapid miniprep method for the preparation of yeast mitochondrial DNA. *Nucl Acids Res* **19:** 185.

Finn RD, Bateman A, Clements J, *et al*. (2014) Pfam: the protein families database. *Nucleic Acids Res* **42:** D222-D230.

Ganguli D, Kumar C & Bachhawat AK (2007) The alternative pathway of glutathione degradation is mediated by a novel protein complex involving three new genes in *Saccharomyces cerevisiae*. *Genetics* **175:** 1137-1151.

724 Gari E, Piedrafita L, Aldea M & Herrero E (1997) A set of vectors with a tetracycline-
725 regulatable promoter system for modulated gene expression in *Saccharomyces cerevisiae*.
726 *Yeast* **13:** 837-848.
727
728 Godard F, Tetaud E, Duvezin-Caubet S & di Rago JP (2011) A genetic screen targeted on the
729 FO component of mitochondrial ATP synthase in *Saccharomyces cerevisiae*. *J Biol Chem*
730 **286:** 18181-18189.
731
732 Goffeau A; Barrell BG; Bussey H; *et al.* (1996) Life with 6000 Genes. *Science* **274:** 563–567.
733
734 Grant CM, Perrone G & Dawes, IW (1998) Glutathione and catalase provide overlapping
735 defenses for protection against hydrogen peroxide in the yeast *Saccharomyces cerevisiae*.
736 *Biochem Biophys Res Commun* **253:** 893–898.
737
738 Handy DE & Loscalzo J (2012) Redox Regulation of Mitochondrial Function. *Antiox Redox*
739 *Sign* **16:** 1323-1367.
740
741 Hildebrand A, Remmert M, Biegert A & Söding J (2009) Fast and accurate automatic
742 structure prediction with HHpred. *Proteins* **77:** 128-132.
743
744 Hiraku M, Murata, S. Kawanishi (2002) Determination of intracellular glutathione and thiols
745 by high performance liquid chromatography with a gold electrode at the femtomole level:
746 comparison with a spectroscopic assay. *Biochim Biophys Acta* **1570:** 47-52.
747

748 Izawa S, Inoue Y & Kimura A (1995) Oxidative stress in yeast: effect of glutathione on
749 adaptation to hydrogen peroxide stress in *Saccharomyces cerevisiae*. *FEBS Lett* **368:** 73–76.
750
751 Jain A; Martensson J; Stole E; Auld PAM & Meister A (1991) Glutathione deficiency leads to
752 mitochondrial damage in brain. *Proc Natl Acad Sci USA* **88:** 1913–1917.
753
754 Jamieson DJ (1998) Oxidative stress responses of the yeast *Saccharomyces cerevisiae*. *Yeast*
755 **14:** 1511–1527.
756
757 Kneer R, Kutchan TM, Hochberger A & Zenk MH (1992) *Saccharomyces cerevisiae* and
758 *Neurospora crassa* contain heavy metal sequestering phytochelatin. *Arch Microbiol* **157:**
759 305–310.
760
761 Kurlandzka A, Rytka J, Gromadka R & Murawski M (1995) A new essential gene located on
762 *Saccharomyces cerevisiae* chromosome IX. *Yeast* **11:** 885-890.
763
764 Laemmli UK (1970) Cleavage of structural proteins during the assembly of the head of bacteriophage
765 T4. *Nature* **227:** 680–685.
766
767 Lee JC, Straffon MJ, Jang TY, Higgins VJ, Grant CM & Dawes IW (2001) The essential and
768 ancillary role of glutathione in *Saccharomyces cerevisiae* analysed using a grande gsh1
769 disruptant strain. *FEMS Yeast Res* **1:** 57-65.
770
771 Lin MT & Beal MF (2006) Mitochondrial dysfunction and oxidative stress in
772 neurodegenerative diseases. *Nature* **443:** 787–795.
773

774 Lindegren CC & Lindegren G (1973) Mitochondrial modification and respiratory deficiency
775 in the yeast cell caused by cadmium poisoning. *Mutation Res* **21:** 315–322.
776
777 Lopez E, Arce C, Oset-Gasque MJ *et al.* (2006) Cadmium induces reactive oxygen species
778 generation and lipid peroxidation in cortical neurons in culture. *Free Radic Biol Med* **40:**
779 940–951.
780
781 Luikenhuis S, Perrone G, Dawes IW & Grant CM (1998) The yeast *Saccharomyces*
782 *cerevisiae* contains two glutaredoxin genes that are required for protection against reactive
783 oxygen species. *Mol Biol Cell* **9:** 1081-1091.
784
785 Madeo F, Fröhlich E, Ligr M, Grey M, Sigrist SJ, Wolf DH, & Fröhlich KU (1999) Oxygen
786 stress: a regulator of apoptosis in yeast. *J Cell Biol* **145:** 757-767.
787
788 Marsella L, Sirocco F, Trovato A, Seno F & Tosatto SC (2009) REPETITA: detection and
789 discrimination of the periodicity of protein solenoid repeats by discrete Fourier transform.
790 *Bioinformatics* **25:** i289-i295.
791
792 Martensson J; Lai JCK & Meister A (1990) High-affinity transport of glutathione is part of a
793 multicomponent system essential for mitochondrial function. *Proc Natl Acad Sci USA* **87:**
794 7185–7189.
795
796 Meister A & Anderson ME (1983) Glutathione. *Annu Rev Biochem* **52:** 711-760.
797

798 Meister A (1995) Mitochondrial changes associated with glutathione deficiency. *Biochim*
799 *Biophys Acta* **1271:** 35-42.
800
801 Mortimer RK & Johnston JR (1986) Genealogy of principal strains of the yeast genetic stock
802 center. *Genetics* **113:** 35-43.
803
804 Namy O, Duchateau-Nguyen G, Hatin I, Hermann-Le Denmat S, Termier M, & Rousset JP
805 (2003) Identification of stop codon readthrough genes in *Saccharomyces cerevisiae*. *Nucleic*
806 *Acids Res* **31:** 2289-2296.
807
808 Ostergaard H, Tachibana C & Winther JR (2004) Monitoring disulfide bond formation in the
809 eukaryotic cytosol. *J Cell Biol* **166:** 337–345.
810
811 Pagni M, Ioannidis V, Cerutti L, Zahn-Zabal M, Jongeneel CV, Hau J, Martin O, Kuznetsov
812 D & Falquet L (2007) MyHits: improvements to an interactive resource for analyzing protein
813 sequences. *Nucleic Acids Res* **32:** W433-W437.
814
815 Perrone GG, Grant CM & Dawes IW (2005) Genetic and environmental factors influencing
816 glutathione homeostasis in *Saccharomyces cerevisiae*. *Mol Biol Cell* **16:** 218-230.
817
818 Petrova VY & Kujumdzieva AV (2010) Robustness of *Saccharomyces cerevisiae* genome to
819 antioxidative stress. *Biotechnology & Biotechnological Equipment* **24:** 474-483.
820
821 Ptacek J, Devgan G, Michaud G, *et al*. (2005) Global analysis of protein phosphorylation in
822 yeast. *Nature* **438:** 679-684.

Ralser M, Kuhl H, Ralser M, Werber M, Lehrach H, Breitenbach M & Timmermann B (2012) The *Saccharomyces cerevisiae* W303-K6001 cross-platform genome sequence: insights into ancestry and physiology of a laboratory mutt. *Open Biol* **2:** 120093. doi: 10.1098/rsob.120093.

Rose M, Winston F & Hieter P (1990) *Methods in Yeast Genetics*. Cold Spring Harbor Laboratory Press, New York.

Schafer FQ & Buettner GR (2001) Redox environment of the cell as viewed through the redox state of the glutathione disulfide/glutathione couple. *Free Radic Biol Med* **30:** 1191–1212.

Shadel GS (1999) Yeast as a model for human mtDNA replication. *Am J Hum Genet* **65:** 1230–1237.

Sharma KG, Kaur R & Bachhawat AK (2003) The glutathione-mediated detoxification pathway in yeast: an analysis using the red pigment that accumulates in certain adenine biosynthetic mutants of yeasts reveals the involvement of novel genes. *Arch Microbiol* **180:** 108-117.

Sian J, Dexter DT, Lees AJ, Daniel S, Agid Y, Javoy-Agid F, Jenner P & Marsden CD (1994) Alterations in glutathione levels in Parkinson's disease and other neurodegenerative disorders affecting basal ganglia. *Annu Neurol* **36:** 348–355.

Sofic E; Lange KW; Jellinger K & Riederer P (1992) Reduced and oxidized glutathione in the substantia nigra of patients with Parkinson's disease. *Neurosci Lett* **142:** 128–130.

Ströher E & Millar AH (2012) The biological roles of glutaredoxins. *Biochem J* **446:** 333-348.

Suzuki T, Yokoyama A, Tsuji T, Ikeshima E, Nakashima K, Ikushima S, Kobayashi C & Yoshida A (2011) Identification and characterization of genes involved in glutathione production in yeast. *J Biosci Bioeng* **112:** 107-113.

Szklarczyk R & Heringa J (2004) Tracking repeats using significance and transitivity. *Bioinformatics* **20:** i311-i317.

Tamas MJ, Labarre J, Toledano MB & Wysocki R (2006) Mechanisms of toxic metal tolerance in yeast. *Top Curr Genet* **14:** 395–454.

Tan SX, Greetham D, Raeth S, Grant CM, Dawes IW& Perrone GG (2010) The thioredoxin-thioredoxin reductase system can function in vivo as an alternative system to reduce oxidized glutathione in *Saccharomyces cerevisiae*. *J Biol Chem* **285:** 6118-6126.

Tarassov K, Messier V, Landry CR, Radinovic S, Serna Molina MM, Shames I, Malitskaya Y, Vogel J, Bussey H & Michnick SW (2008) An in vivo map of the yeast protein interactome. *Science* **320:** 1465-1470.

872 Thévenod F (2009) Cadmium and cellular signaling cascades: To be or not to be? *Toxicol*
873 *Appl Pharmacol* **238:** 221–239.
874
875 Thomas BJ & Rothstein R (1989). Elevated recombination rates in transcriptionally active
876 DNA. *Cell* **56:** 619–630.
877
878 Tóth A, Ciosk R, Uhlmann F, Galova M, Schleiffer A & Nasmyth K (1999) Yeast cohesin
879 complex requires a conserved protein, Eco1p(Ctf7), to establish cohesion between sister
880 chromatids during DNA replication. *Genes Dev* **13:** 320-333.
881
882 Turton HE, Dawes IW & Grant CM (1997) *Saccharomyces cerevisiae* exhibits a yAP-1-
883 mediated adaptive response to malondialdehyde. *J Bacteriol* **179:** 1096–1101.
884
885 Turrens JF (2003) Mitochondrial formation of reactive oxygen species. *J Physiol* **552:** 335–
886 344.
887
888 Wallace DC (2005) A mitochondrial paradigm of metabolic and degenerative diseases, aging,
889 and cancer: a dawn for evolutionary medicine. *Annu Rev Genet* **39:** 359-407.
890
891 Wallace DC & Fan W (2010) Energetics, epigenetics, mitochondrial genetics. *Mitochondrion*
892 **10:** 12-31.
893
894 Winiarska K, Drozak J, Wegrzynowicz M, Jagielski AK & Bryla J (2003) Relationship
895 between gluconeogenesis and glutathione redox state in rabbit kidney-cortex tubules.
896 *Metabolism* **52:** 739-746.

Wojas S, Clemens S, Hennig J, Sklodowska A, Kopera E, Schat H, Bal W & Antosiewicz DM (2008) Overexpression of phytochelatin synthase in tobacco: distinctive effects of AtPCS1 and CePCS genes on plant response to cadmium. *J Exp Bot* **59:** 2205–2219.

Wunschmann J, Beck A, Meyer L, Letzel T,Grill E &, Lendzian KL (2007) Phytochelatins are synthesized by two vacuolar serine carboxypeptidases in *Saccharomyces cerevisiae*. *FEBS Lett* **581:** 1681–1687.

Wysocki R & Tamas MJ (2010) How *Saccharomyces cerevisiae* copes with toxic metals and metalloids. *FEMS Microbiol Rev* **34:** 925-951.

908 # Tables

909 **Table 1.** *S. cerevisiae* strains

Strain	Description	Genotype	Source
IMI1	W303-1A, wild-type	*MAT* **a** *ade2-1 his3-11,15 leu2-3,112 trp1-1 ura3-1 can1-100*	Rothstein collection (Columbia University, New York, USA)
imi1Δ	W303-1A derivative	*MAT* **a** *ade2-1 his3-11,15 leu2-3,112 trp1-1 ura3-1 can1-100 imi1::kanMX6*	This study
imi1Δ[*rho*$^{+}$(W303)]	*imi1Δ* containing mitochondria derived from W303	*MAT* **a** *ade2-1 his3-11,15 leu2-3,112 trp1-1 ura3-1 can1-100 imi1::kanMX6* [mtDNA *rho*$^{+}$]	This study
MR6/b-3	W303 derivative, [*rho*^{0}]	*MAT α ade2–1 his3–11,15 leu2–3,112 trp1–1 ura3–1 CAN1 arg8::HIS3* [*rho*^{0}]	Godard *et al*., (2011)

910

911 **Table 2.** Plasmids used in this study

Plasmid	Description
pGEM-*IMI1*	Amp^R, derivative of pGEM-T Easy (Promega)
P_{IMI1}-*IMI1*	*URA3*, Amp^R, centromeric (derivative of pRS316)
P_{IMI1}-*IMI1-RFP*	*URA3*, Amp^R, centromeric, (derivative of pUG35)
P_{tetO}-*IMI1-RFP*	*URA3*, Amp^R, centromeric, (derivative of pCM189)
P_{tetO}-*IMI1*	*URA3*, Amp^R, centromeric, (derivative of pCM189)

912

913